

Photothermal detection of magnetic polaritons in FeF₂

R. M. Toussaint and V. Jaccarino

Citation: *Journal of Applied Physics* **55**, 2458 (1984); doi: 10.1063/1.333694

View online: <http://dx.doi.org/10.1063/1.333694>

View Table of Contents: <http://scitation.aip.org/content/aip/journal/jap/55/6?ver=pdfcov>

Published by the *AIP Publishing*

Articles you may be interested in

[Magnetic ordering in dimorphic phases of FeF₃·3H₂O: Magnetic and Mössbauer studies](#)

J. Appl. Phys. **61**, 4346 (1987); 10.1063/1.338443

[ELECTRONIC RAMAN SCATTERING IN FeF₂](#)

AIP Conf. Proc. **5**, 344 (1972); 10.1063/1.3699453

[High-Low-Temperature Static Magnetic Properties of FeF₂](#)

J. Appl. Phys. **42**, 1499 (1971); 10.1063/1.1660318

[Measurement of Dynamical Scaling in FeF₂](#)

J. Appl. Phys. **42**, 1376 (1971); 10.1063/1.1660256

[Correlation of Magnetic Susceptibility and Infrared Spectra of FeF₂](#)

J. Appl. Phys. **39**, 1141 (1968); 10.1063/1.1656201



Powerful, Multi-functional UV-Vis-NIR and FTIR Spectrophotometers

Providing the utmost in sensitivity, accuracy and resolution for applications in materials characterization and nano research

- Photovoltaics
- Polymers
- Thin films
- Paints
- Ceramics
- DNA film structures
- Coatings
- Packaging materials

[Click here to learn more](#)



Photothermal detection of magnetic polaritons in FeF₂

R. M. Toussaint^{a)} and V. Jaccarino

Department of Physics, University of California, Santa Barbara, California 93106

The technique of photothermal detection has been extended to the FIR and used, in conjunction with a high-resolution FIR-laser spectrometer, to directly measure the absorption spectra of antiferromagnetic FeF₂. Samples of various thicknesses were studied and the results successfully compared to computer generated spectra of magnetic polaritons—the propagating coupled photon-magnon modes. Spectra for the downgoing branch were taken at a fixed frequency of $\nu = 1.3623$ THz with $\mathbf{H}_0 \parallel \hat{c}$. In addition to the expected peak associated with the FeF₂ AFMR, a second, smaller peak appears at a slightly higher magnetic field. This double peak structure is shown to be characteristic of magnetic polaritons, with the second peak corresponding to the upper boundary of the polariton “forbidden band.” Both the intensity and width of this second peak are particularly sensitive indicators of the intrinsic AFMR linewidth.

PACS numbers: 75.50.Ee, 78.20.Ls, 75.30.Ds

MAGNETIC POLARITONS

In far-infrared laser studies of the AFMR of FeF₂, unusually broad, asymmetric transmission spectra have been observed. A considerable amount of success has resulted from identifying this mode as a magnetic polariton—the propagating coupled photon-magnon mode.^{1,2,3} The model is essential to understanding the intrinsic linewidth contributions since the apparent width of the AFMR is largely determined by the magnetic polariton dispersion, rather than by intrinsic relaxation processes. The magnetic polariton model is thoroughly discussed in Refs. 2 and 4; only a brief description of it is given here.

The basis of the polariton model is an effective-field, coupled-equations of motion approach. It yields the frequency- and field-dependent transverse susceptibility of an uniaxial AF with an applied magnetic field H_0 parallel to the unique axis and driven by a perpendicular rotating field of frequency ω :

$$\chi^\pm(\omega, H_0) = 2H_A \frac{M}{2H_E H_A + H_A^2 - (\omega/\gamma \pm H_0)^2}. \quad (1)$$

Here γ is the gyromagnetic ratio, H_A (H_E) is the anisotropy (exchange) field, and M is the sublattice magnetization. Since the wavelength of the exciting electromagnetic radiation in FeF₂ is comparable to typical sample dimensions ($\lambda \approx 0.1$ mm in FeF₂), propagation through the sample must be considered. After introducing the susceptibility tensor, the following polariton dispersion is obtained

$$k^\pm = \frac{\omega}{c} \sqrt{\epsilon} \left\{ 1 + 8\pi M \frac{H_A}{2H_E H_A + H_A^2 - (\omega/\gamma \pm H_0)^2} \right\}^{1/2}, \quad (2)$$

where ϵ is the dielectric constant and c is the speed of light in the vacuum. Equation (2) is plotted for $H_0 = 0$ in Fig. 1 and shows the characteristic polariton dispersion (analogous to the more familiar phonon-photon case).

The transmission, reflection, and absorption coefficients necessary to make detailed comparison between theory and experiment were calculated for the case of radiation normally incident upon a dielectric slab with parallel faces. ϵ

is taken to be isotropic and real, whereas n and μ are allowed to be complex.

Calculated transmission, reflection, and absorption spectra of FeF₂ with $t = 100 \mu\text{m}$, $\Delta H = 100$ Oe are compared to the magnetic polariton dispersion in Fig. 2 (analytic expressions for T , R , and A are given in Ref. 3). To simulate experimental conditions, the frequency is held constant ($\nu = 1.3623$ THz) and the applied magnetic field H_0 is varied. The importance of the forbidden band in the study of AFMR linewidths can now be seen. Transmission is strongly attenuated for frequencies within the forbidden band, where k is pure imaginary. This produces a line profile with an apparent width not determined by the intrinsic relaxation processes but, in large part, by the forbidden band itself.

By comparison with the polariton dispersion (calculated from Eq. (2) using parameters appropriate to FeF₂⁵), the important spectral features (A–G) can be easily understood. (Although the transmission spectrum associated with magnetic polaritons has been thoroughly discussed in Ref. 2, it is reviewed here for clarity).

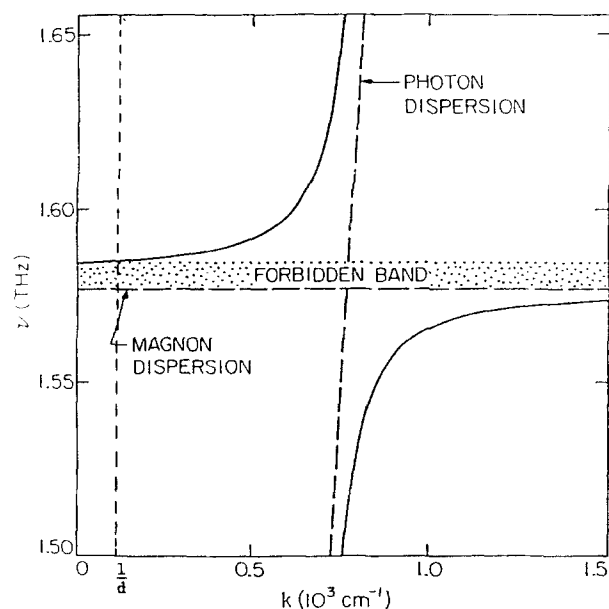


FIG. 1. Calculated magnetic polariton dispersion in FeF₂.

^{a)} Formerly R. M. Belanger.

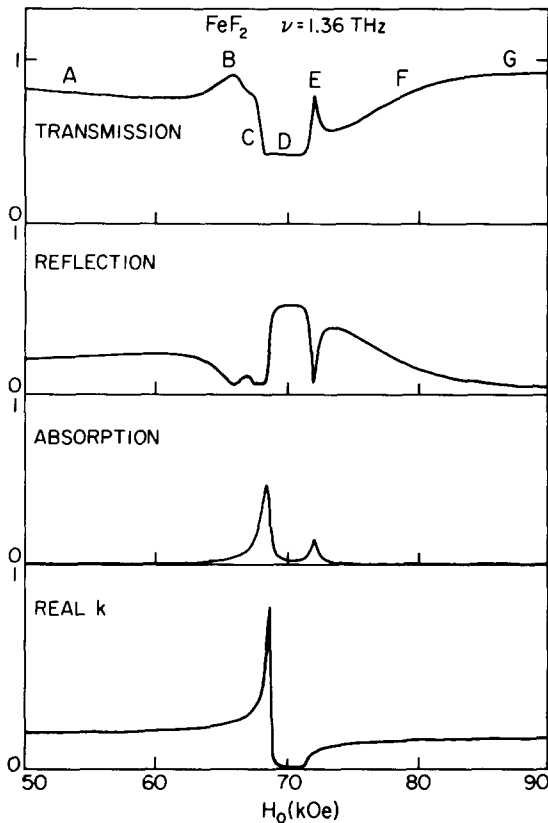


FIG. 2. Calculated spectra characteristic of magnetic polaritons in FeF_2 . The features A–G are discussed in the text.

Far off resonance (A,G) the wave vector k is entirely real and varies slowly with H_0 . Therefore, the transmission, which depends on thickness t and k , is almost constant. Approaching the resonance position (from either side), $\text{Re } k$ varies rapidly and gives rise to the interference peaks which are labeled by B and F. At the resonance position, the imaginary component of k , $\text{Im } k$, varies from zero to its maximum value, causing the sharp slope in the transmission spectrum labeled C. The low-field corner corresponds to the AFMR position for the lower branch where the “–” polarization radiation is completely absorbed, as is easily seen by a comparison of the three spectra. The first peak (low-field) in the absorption spectra, which is saturated at 50% for unpolarized incident radiation, coincides with the peak in $\text{Im } k^-$. This peak in the absorption occurs only for finite linewidth. The flat portion of the transmission curve at D is a consequence of the forbidden band. Since the extinction coefficient depends on $\exp(-\text{Im } k^- \cdot t)$, transmission in the forbidden band is a function of both wavevector and thickness. Therefore, for a given value of t , there is a range of $\text{Im } k^-$ where the “–” polarization is almost completely absorbed (at $t \sim 1/\text{Im } k^-$).

In this region D, where the reflectance is at a maximum, there is little transmitted light to be absorbed, and the absorption vanishes. The point labeled E corresponds to the point where both $\text{Re } k$ and $\text{Im } k$ are small. Here there is an abrupt maximum in the transmission and a minimum in the reflection (see Fig. 2). Accordingly, if the AFMR has a finite linewidth such that $\text{Im } \chi^-$ is finite at the point labeled E, there will be a second peak in the absorption. Both the inten-

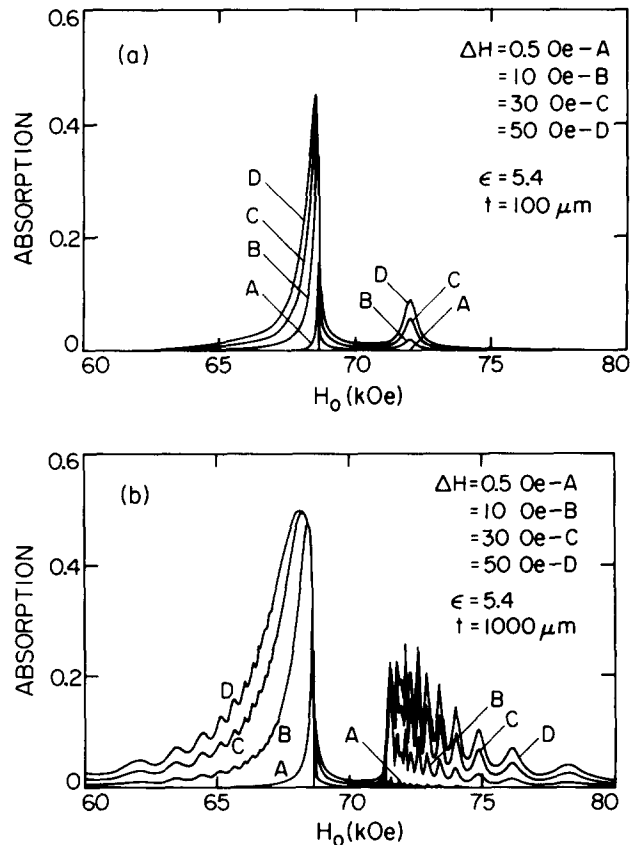


FIG. 3. Calculated absorption spectra of FeF_2 for (a) a thin and (b) a thick sample. The sensitivity of the spectra to small variations of ΔH is shown.

sity and width of this “second peak” are sensitive indicators of the AFMR linewidth. The sensitivity of the calculated absorption spectrum of a thin sample ($t = 100 \mu\text{m}$) to small variations in ΔH is shown in Fig. 3(a). Notice the apparent absence of the “second peak” for $\Delta H = 0.5$ Oe, as is to be expected, although there is complete transmission of “–” polarized radiation through the sample at the top of the forbidden band (H_L), $\Delta H \simeq 0$ at this point. It follows that there can be little absorption at $H = H_L$. The sensitivity of the absorption spectrum of a thick sample ($t = 1000 \mu\text{m}$) to small variation in ΔH is shown in Fig. 3(b). Notice the complex structure visible in the thick-sample spectra. Since consecutive local extrema in transmission correspond to changes of π/t in $\text{Re } k$, at t increases the number of interference structures also increase.³

EXPERIMENTAL APPARATUS

Direct transmission and absorption measurements at 4.2 K of the AFMR spectra were made with a far-infrared (FIR) laser-superconducting solenoid spectrometer. With the exception of the photothermal detector, the apparatus is described elsewhere.^{2,5}

In addition to direct transmission measurements, photoacoustic^{6,7} and photothermal detection are useful techniques in the FIR. The basic idea of photothermal detection is to directly observe the radiation absorbed by a sample by measuring its temperature rise. Since on resonance, FeF_2 absorbs half of the unpolarized incident power and the lattice specific heat is very small at 4.2 K, one expects a substan-

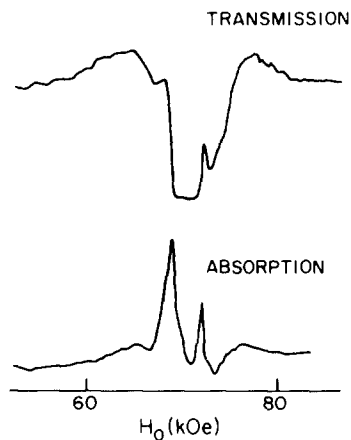


FIG. 4. Observed transmission and absorption spectra of 1.3623 THz radiation for a 106 ± 2 - μm -thick sample of FeF_2 .

tial temperature rise. The temperature sensing element used is a cylindrical carbon cryogenic thermistor (Model L0904-25K-HE-T2, Keystone Carbon Co.), approximately 0.1 in. in diameter and 0.04 in. thick. At liquid He temperature, it has a resistance of 25 k Ω , and a temperature coefficient of $\sim -300\%/1^\circ\text{C}$. The sensing element is attached to the back of a small copper foil iris with indium solder. A sample, typically 6 mm in diameter and 100–500 μm thick, is attached to the front of the iris with a thin layer of silicon grease. In the sample space, conduction between the detector and the heat reservoir is mediated by the He gas. Conditions are optimum for a power chopping frequency of ~ 17 Hz and a He gas pressure of ~ 1000 μm Hg. A 9- μA current source was provided by a 9-V battery in series with a 1-M Ω resistor. For incident laser power of $\sim 1/2$ mW, a typical absorption signal of 500 μV is measured.

Spectra were obtained at a fixed frequency of $\nu = 1.3623$ THz (H_2O vapor laser line) by sweeping the external magnetic field H_0 , applied parallel to the unique (\hat{c}) axis of the crystal. The radiation ($\mathbf{h}||\hat{c}$) was incident normal to the faces (polished with a 1 μm finish) of disk-shaped samples.

EXPERIMENTAL OBSERVATIONS

Observed transmission and absorption spectra for a 106- μm -thick sample of FeF_2 are shown in Fig. 4 ($\nu = 1.3623$ THz, $\mathbf{H}_0||\hat{c}$).⁵ The transmission spectrum exhibits the broad, asymmetric line profile, characteristic of magnetic polaritons, and the absorption spectrum clearly shows two peaks, one at either edge of the forbidden band, as predicted by the magnetic polariton model. Figure 5 shows measured absorption spectra ($\nu = 1.3623$ THz $\mathbf{H}_0||\hat{c}$) for three different thicknesses of a 0.01 at. % Mn sample of $\text{Mn}:\text{FeF}_2$. The model predictions use $\Delta H = 50$ Oe as well as

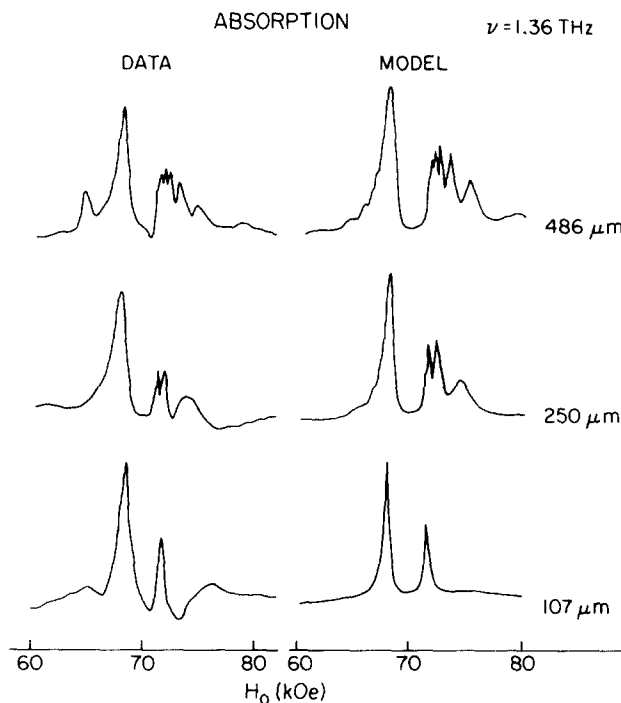


FIG. 5. Observed absorption spectra for several thicknesses of a 0.01% $\text{Mn}:\text{FeF}_2$ sample compared to the polariton model with $H = 50$ Oe. Excellent agreement is obtained from a frequency-dependent two-magnon, exchange (J'') coupled, impurity scattering mechanism.

the two-magnon impurity scattering linewidth appropriate for $\text{FeF}_2:\text{Mn}$ (Ref. 8) with $J'_1 = 0.2 \text{ cm}^{-1}$, $J'_2 = 1.79 \text{ cm}^{-1}$ and $c = 0.01\%$ Mn. Only the thickness was changed between fits. It is clear that the intensity and width of the peak at the top of the forbidden band is particularly sensitive to the intrinsic AFMR linewidth.

We thank N. Nighman for the growth of the crystal and the National Science Foundation for support through grant No. DMR80-17582.

¹R. W. Sanders, V. Jaccarino, and S. M. Rezende, *Solid State Commun.* **28**, (1978) 907.

²R. W. Sanders, R. M. Belanger, M. Motokawa, V. Jaccarino, and S. M. Rezende, *Phys. Rev. B*, **23**, 1190 (1981).

³R. M. Belanger, V. Jaccarino, and S. Geschwind, *J. Magn. Magn. Mater.* **31-34**, 681 (1983).

⁴D. L. Mills and E. Burstein, *Rep. Prog. Phys.* **37**, 817 (1974).

⁵R. M. Toussaint, Ph.D. thesis, University of California, Santa Barbara, 1982 (unpublished).

⁶C. K. N. Patel and A. C. Tam, *Rev. Mod. Phys.* **53**, 517 (1981).

⁷M. Davies (unpublished).

⁸R. M. Toussaint, S. M. Rezende, D. Hone, and V. Jaccarino (unpublished).